Inorganic Chemistry
Communication

Inorg. Chem. **2010**, *49*, 6393–6395 **6393**
DOI: 10.1021/ic101016t

Isostructural Single-Chain and Single-Molecule Magnets

Patrick L. Feng and David N. Hendrickson*

Department of Chemistry and Biochemistry, University of California, San Diego, La Jolla, California 92093-0358

Received May 20, 2010

Isostructural single-chain magnet (SCM) and single-molecule magnets (SMM) with formulas $[Mn_6X_2(salox)_6O_2(N_3)_8]$ (X = Mn^{II} (**1**), Cd^{II} (**2**); H_2salox = salicylaldoxime) have been synthesized and magnetically characterized. Complexes **1** and **2** possess significantly different magnetization reversal barriers of U_{eff} = 100.3 and 57.0 K, in spite of comparable uniaxial anisotropies (D) and ground state spin values (S). These observations are indicative of the intrinsic spin dynamics in these structurally related yet magnetically distinct SCM/SMM systems.

Nanoscale molecular-based magnetic materials have attracted significant interest due to the unique finite-size and quantum mechanical properties they possess.[1−9] Among this class of materials are single-molecule magnets (SMMs), which are discrete molecular clusters that exhibit superparamagnetic-like behavior as a result of the combination of an appreciable ground state spin and uniaxial (Ising) molecular anisotropy.[2] SMMs have served as an exceptional test bed for studying fundamental quantum magnetic phenomena, including quantum tunneling of the magnetization (QTM),[2] quantum phase interference,[6] and quantum coherence,[10] among others.

Single-chain magnets (SCMs) comprise another class of molecule-based magnets that also exhibit slow magnetization relaxation.[8,9] The barrier to magnetization reversal in these materials is no longer the sole consequence of a high-spin ground state and uniaxial anisotropy but is also due to the 1-D magnetic correlations along the chain.[11] Consequently, no quantum effects are observed in SCMs.

To gain insight toward the transition from quantum to classical behavior in SMMs and SCMs, respectively, a number of groups including our own have synthesized 1-D systems comprising discrete SMM subunits.[12,13] In these studies, the differences in relaxation times and hysteresis loops were investigated, indicating the interplay between anisotropy, intrachain magnetic exchange, and finite-size effects.

Herein we describe the complexes $[Mn_8(salox)_6O_2(N_3)_6(MeOH)_4]_\infty$ (**1**) and $[Mn_6Cd_2(salox)_6O_2(N_3)_6(MeOH)_4]_\infty$ (**2**), which are azide-bridged 1-D chains based on the molecular SMM subunits $[NPr_4]_2[Mn_8(salox)_6O_2(N_3)_6(MeOH)_2Cl_2]\cdot 2CHCl_3$ (**3**) and $[NPr_4]_2[Mn_6Cd_2(salox)_6O_2(N_3)_6(MeOH)_2I_2]\cdot 2MeOH$ (**4**). Complexes **1** and **2** are unique in that they are crystallographically isomorphic and coordinatively isostructural, allowing for direct comparisons between the relaxation dynamics in a SCM and a related chain of diamagnetically separated SMMs. Complexes **1** and **2** are the subject of this study, with **3** and **4** presented in the Supporting Information. Structures based on similar building blocks have been previously reported.[14−16]

Complexes **1**−**4** may be described as two planar, offset Mn_3^{III} triangles that are capped by two Mn^{II} or Cd^{II} ions. Each Mn_3^{III} triangle comprises a centered planar μ_3-oxo and three doubly deprotonated salicylaldoxime chelating groups, resulting in a near-parallel arrangement of the Mn^{III} single-ion Jahn−Teller (JT) elongation axes. Oximate linkages

*To whom correspondence should be addressed. E-mail: dhendrickson@ucsd.edu. Fax: 858-534-5383.

(1) Sessoli, R.; Tsai, H.-L.; Schake, A. R.; Wang, S.; Vincent, J. B.; Folting, K.; Gatteschi, D.; Christou, G.; Hendrickson, D. N. *J. Am. Chem. Soc.* **1993**, *115*, 1804.
(2) Sessoli, R.; Gatteschi, D.; Caneschi, A.; Novak, M. A. *Nature* **1993**, *365*, 141.
(3) Thomas, L.; Lionti, F.; Ballou, R.; Gatteschi, D.; Sessoli, R.; Barbara, B. *Nature* **1996**, *383*, 145.
(4) Wernsdorfer, W.; Aliaga-Alcalde, N.; Hendrickson, D. N.; Christou, G. *Nature* **2002**, *416*, 406.
(5) Hill, S.; Edwards, E. S.; Aliaga-Alcalde, N.; Christou, G. *Science* **2003**, *302*, 1015.
(6) Wernsdorfer, W.; Bhaduri, S.; Boskovic, C.; Christou, G.; Hendrickson, D. N. *Phys. Rev. B* **2002**, *65*, 180403.
(7) Gatteschi, D.; Caneschi, A.; Pardi, L.; Sessoli, R. *Science* **1994**, *265*, 1054.
(8) Clerac, R.; Miyasaka, H.; Yamashita, M.; Coulon, C. *J. Am. Chem. Soc.* **2002**, *124*, 12837.
(9) Caneschi, A.; Gatteschi, D.; Lalioti, N.; Sangragorio, C.; Sessoli, R.; Venturi, G.; Vindigni, A.; Rettori, A.; Pini, M. G.; Novak, M. A. *Angew. Chem., Int. Ed.* **2001**, *40*, 1760.
(10) Takahashi, S.; van Tol, J.; Beedle, C. C.; Hendrickson, D. N.; Brunel, L.-C.; Sherwin, M. S. *Phys. Rev. Lett.* **2009**, *102*, 087603.
(11) Glauber, R. J. *J. Math Phys.* **1963**, *4*, 294.
(12) Ferbinteanu, M.; Miyasaka, H.; Wernsdorfer, W.; Nakata, K.; Sugiura, K.; Yamashita, M.; Coulon, C.; Clerac, R. *J. Am. Chem. Soc.* **2005**, *127*, 3090.
(13) Yoo, J.; Wernsdorfer, W.; Yang, E.-C.; Nakano, M.; Rheingold, A. L.; Hendrickson, D. N. *Inorg. Chem.* **2005**, *44*, 3377.
(14) (a) Milios, C. J.; Inglis, R.; Vinslava, A.; Prescimone, A.; Parsons, S.; Perlepes, S. P.; Christou, G.; Brechin, E. K. *Chem. Commun.* **2007**, 2738. (b) Milios, C. J.; Piligkos, S.; Brechin, E. K. *Dalton Trans.* **2008**, 1809.
(15) Yang, C.-I.; Wernsdorfer, W.; Lee, G.-H.; Tsai, H.-L. *J. Am. Chem. Soc.* **2007**, *129*, 456.
(16) Feng, P. L.; Koo, C.; Henderson, J. J.; Nakano, M.; Hill, S.; del Barco, E.; Hendrickson, D. N. *Inorg. Chem.* **2008**, *47*, 8610.

Published on Web 06/21/2010

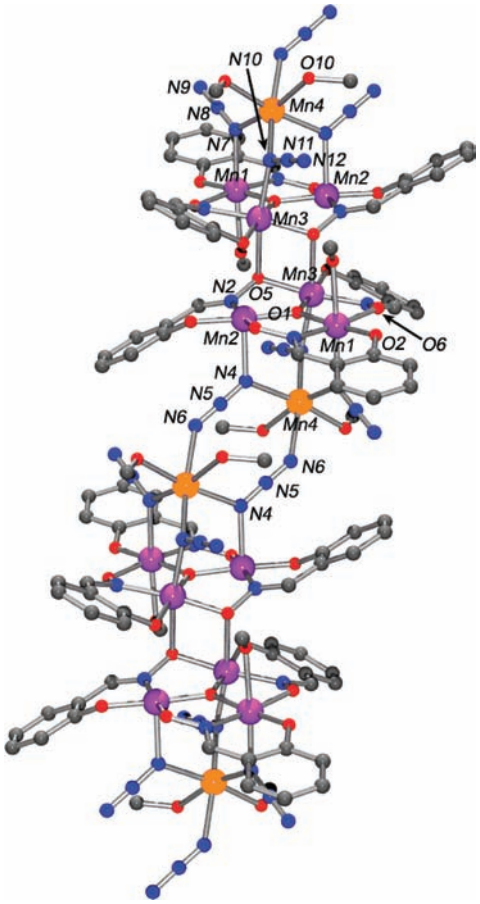

Figure 1. Structure of complex **1**, shown as a ball-and-stick model, for clarity. Purple spheres depict Mn^{III} ions while orange spheres indicate Mn^{II} ions in **1** and Cd^{II} ions in **2**.

straddle crystallographic inversion centers and bridge the two Mn_3^{III} triangles in an arrangement that further supports the relative alignment of single-ion JT axes. These structures are further characterized by apical divalent metal ions that are coordinated to the Mn^{III} ions through three $\mu_{1,1}$-azides, one of which also serves as an end-to-end $\mu_{1,3}$-azide bridge between neighboring $Mn_6^{III}M_2^{II}$ clusters. Complex **1** is closely related to **3** where the primary difference is the change of divalent ion coordination geometry, from tetrahedral to octahedral. This change in geometry is accompanied by replacement of the terminal halide ion by two $\mu_{1,3}$-azide bridging ligands and the corresponding exclusion of both $[NPr_4]^+$ counterions. A similar relationship is observed between the $Mn_6^{III}Cd_2^{II}$ complexes **2** and **4**.

Complexes **1** and **2** (Figure 1) were synthesized from reactions of the respective Mn^{II} and Cd^{II} nitrates with NaN_3 and salicylaldoxime in MeOH, crystallizing in the triclinic space group $P\bar{1}$ as large blocks over 3 days in 65−75% yield. Dc susceptibility measurements on **1** indicate a complex magnetic behavior, as evident from the temperature- and field-dependent susceptibility from 0.01−1 T and at 300−1.8 K. At all of the fields tested, the smooth decrease in $\chi_M T$ from 300−30 K is indicative of dominant antiferromagnetic interactions along the chain. The 0.01 T susceptibility below 30 K continues this decrease, reaching a minimum value of 5.55 $cm^3 \cdot K \cdot mol^{-1}$ at 1.8 K. Surprisingly, the low temperature susceptibility data taken at larger fields of 0.1 T and 1 T do not exhibit this behavior but instead increase to maxima of

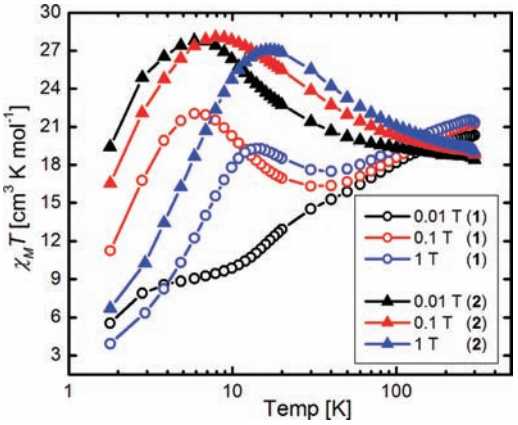

Figure 2. Comparison of the $\chi_M T$ data for complexes **1** and **2** at the fields shown. Solid lines serve as guides for the eyes.

22.03 $cm^3 \cdot K \cdot mol^{-1}$ at 5.84 K and 19.29 $cm^3 \cdot K \cdot mol^{-1}$ at 13.9 K, respectively.

These observations are consistent with a nonzero molecular anisotropy and suggest a possible spin-flop transition at fields larger than 0.01 T, leading to a ferrimagnetic 1-D chain. Unfortunately, fitting of these susceptibility data for **1** was not possible due to overparameterization arising from the low symmetry and presence of numerous exchange pathways. Variable-field magnetization data collected on a powder sample of **1** from 1.8−4 K and at 1−5 T are interesting in that they reveal magnetization saturation even at 1 T and indicate an $S \approx 6$ ground state experiencing significant zero-field splitting (Figure 2). It was not possible to fit these data to a single spin ground state, suggesting the presence of low-lying excited states, as have been previously characterized in related complexes.[14−16] Similar dc susceptibility measurements were conducted on complex **2**, revealing a strong field dependence and dominant ferromagnetic interactions from 300−1.8 K. Least-squares fitting of the variable-field magnetization data indicate an $S = 7$ spin ground state and fitting parameters of $g = 1.87$ and $D = -0.75$ cm^{-1} (Figure S3, Supporting Information). This large axial zfs parameter is consistent with the near-parallel arrangement of individual Mn^{III} Jahn−Teller elongation axes in these complexes.

Ac susceptibility data were collected from 10 to 1000 Hz at 1.8−7 K to compare the relaxation behavior for complexes **1** and **2**. Both complexes exhibit clear peaks in the out-of-phase susceptibility (χ'') and show concomitant decreases in the in-phase susceptibility (χ'), indicating slow magnetization relaxation in this temperature and frequency range (Figures 3 and S4, Supporting Information). Extrapolation of the 10 Hz in-phase susceptibility to 0 K reinforce the $S \approx 6$ (**1**) and $S = 7$ (**2**) ground states determined from the dc susceptibility, while inspection of the temperature and frequency dependence of the χ'' peaks for **1** and **2** reveal clear differences in the magnetization relaxation behavior. Interestingly, the kinetic barrier to magnetization reversal (U_{eff}) for complex **1** is 100.3 K while the barrier in **2** is significantly less at 57.0 K, despite a comparable axial zfs and larger spin ground state in **2**. This variation is directly attributed to the long-range 1-D magnetic correlations in **1** and is best explained in terms of SCM behavior, as mediated by the presence of Mn^{II} ions along the chain. Further evidence for this claim is clear from the calculated maximum thermodynamic barriers of 39 K ($S = 6$) and 53 K ($S = 7$), as approximated by $|D|S_z^2$ for **1** and **2**, respectively.

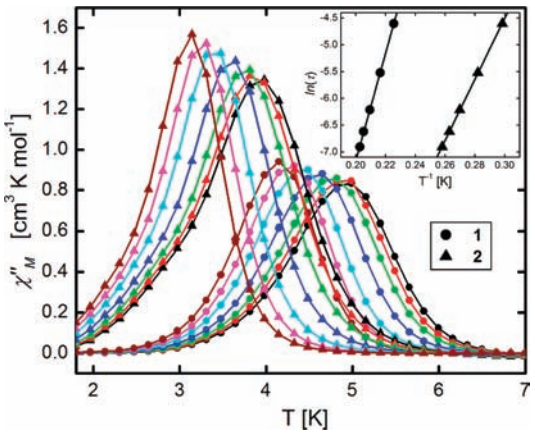

Figure 3. Plot of the out-of-phase susceptibility (χ''_M) from 10 to 1000 Hz for complexes **1** and **2**. The corresponding Arrhenius plot from 100 to 1000 Hz is shown (inset) for parameters discussed in the text.

Another quantity that further differentiates complexes **1** and **2** is the Arrhenius pre-exponential factor τ_0, which describes the intrinsic spin dynamics for a system in contact with a thermal bath, in the absence of an energy barrier. The value of τ_0 for **1** (1.48×10^{-12} s) was found to be nearly 300 times smaller than τ_0 for **2** (4.12×10^{-10} s), indicating a more efficient mechanism for thermal spin fluctuation in **1**. For comparison, τ_0 does not vary by more than a factor of 4 in SMM complexes **2**−**4**. Consequently, the variations in U_{eff} and τ_0 for **1** and **2** affect the relaxation time in opposing ways, serving to minimize differences in the blocking temperature, T_B (at τ = 100 s), which was found to be 0.32 K in **1** and 0.46 K in **2**. These observations highlight fundamental differences in the nature of magnetization relaxation within these structurally related chain systems, as evidenced by the very different Arrhenius behaviors yet comparable blocking temperatures.

Magnetization hysteresis loops were collected at 1.8 K on restrained and partially aligned polycrystalline samples to further assess the nature of magnetization relaxation in **1** and **2**. From first inspection of these data (Figures S5 and S6, Supporting Information), it is apparent that both complexes exhibit magnetization hysteresis, while neither appears to show the vertical steps that are associated with QTM. This observation is consistent with SCM behavior for complex **1**, as variations in correlation length and the formation of domain walls are expected to significantly broaden the features corresponding to quantum phenomena such as QTM. For complex **2**, a plot of dM/dH vs H reveals a small but reproducible acceleration of the magnetization relaxation at zero applied field, as expected for QTM between spin levels with $\Delta|m_s| = 0$. The weakness of this feature may be due to the small percentage of molecules in the powder sample that are exactly aligned with the applied magnetic field (H_z), along with instrumental limitations with respect to temperature and field sweep rate. Work is in progress to study this behavior in an aligned single crystal at lower temperatures and will be reported at a later date.

We thus present two neutral 1-D chain complexes comprising repeating units of discrete Mn_8 and Mn_6Cd_2 SMMs. The targeted replacement of $S = 5/2$ Mn^{II} ions in **1** by diamagnetic Cd^{II} cations (**2**) interrupts the interchain magnetic interactions while also demonstrating the considerable synthetic flexibility afforded in these systems. Remarkably, both 1-D chains exhibit near-identical bond lengths and angles in isomorphous crystal lattices, significantly minimizing differences with respect to intermolecular/interchain interactions as well as intramolecular $Mn^{III}-Mn^{III}$ superexchange. A greatly enhanced (75%) U_{eff} is observed for the SCM complex **1** compared with the SMM complex **2**, combined with an almost 300 times smaller value for τ_0 in **1**. In light of these differences, similar blocking temperatures are observed for both chain complexes, revealing fundamentally different mechanisms for magnetization relaxation. Detailed magnetic and spectroscopic characterizations of these complexes are forthcoming, promising to reveal new insight toward the transition from quantum to classical magnetic behavior.

Acknowledgment. This work was supported by the National Science Foundation.

Supporting Information Available: Crystallographic information in cif format and ORTEP structures, least-squares fit of the reduced magnetization, ac susceptibility data, and magnetization hysteresis loops. This material is available free of charge via the Internet at http://pubs.acs.org.